ORIGINAL ARTICLE

Enhancing Cilnidipine Solubility Using Co-amorphous Formulation with L-Tryptophan: Molecular Docking, Physicochemical Characterization, and Development of Optimized Fast-dissolving Tablets

Gaurang Sharma, Jitendra Gupta

Department of Pharmaceutics, Institute of Pharmaceutical Research, GLA University, Mathura, Uttar Pradesh, India

Abstract

Cilnidipine (CIL), is a calcium channel blocker and a Biopharmaceutics Classification System Class II drug, exhibits poor aqueous solubility. The study aimed to enhance CIL's solubility through the development of a co-amorphous (COAM) system using L-tryptophan (1:1 molar ratio). Molecular docking was employed before formulation to investigate interactions, such as hydrogen bonding, π-π and σ-π stacking, confirming a strong binding affinity between CIL and the amino acids. The COAM system was prepared using the solvent evaporation method, and subsequently characterized using Fourier transform infrared spectroscopy, Differential scanning calorimetry, X-ray powder diffraction, ^{1}H-Nuclear Magnetic Resonance spectroscopy and scanning electron microscopy. COAM formulation significantly improved solubility by 15.75-fold (81.766 ± 0.5 mg/mL) compared to pure CIL (5.19 ± 0.07 mg/mL) attributed to its transformation into an amorphous state, associated decrease in heat flow and protonation effects. Fast-dissolving tablets (FDTs) incorporating the COAM were developed via direct compression and optimized using a Box-Behnken Design to evaluate essential formulation parameters. The FDTs (F1–F15) demonstrated acceptable physicochemical properties, including uniform weight (99.69 ± 7.47–103.87 ± 6.25 mg), hardness (2.48 ± 0.78–2.67 ± 0.56 kg/cm²), friability (<1%), thickness (3.52 ± 0.14–3.59 ± 0.15 mm), drug content (92 ± 0.16–99 ± 0.78%), and disintegration time (61 ± 2.02–87 ± 1.12 s). The optimized formulation (F14) exhibited rapid disintegration (61 ± 2.02 s) and the highest drug release (94.86 ± 0.29%). This research highlights the potential of COAM for improving the delivery of poorly soluble drugs in the pharmaceutical industry.

Key words: Amino acid, cilnidipine, co-amorphous, fast-dissolving tablet, molecular docking

INTRODUCTION

More than 90% of drugs in development and 40% of generic medicinesare found to have low water solubility, which directly influences the absorption rates, bioavailability, and therapeutic efficacy.[1] Biopharmaceutics Classification System (BCS) Class II drugs createsan unique challenge which is low solubility as well as limited absorption which leads to slow dissolution rates. This solubility limitation is required for enhancing the pace and extent of gastrointestinal absorption, hence enhancing therapeutic efficacy.[2] Strategies to improve solubility requires the increase in the dissolution rate or achieving sustained solubility over time.

Several strategies have been developed to address the solubility issues, which include solid dispersions (SD) like amorphous formulations, salt formation, and complexation.[3] Amorphous solid forms are found to be effective as they need low energy for molecular dispersion, which results in improved solubility and faster dissolution rates when compared to crystalline forms of drugs. The reduced particle size and the applications

Address for correspondence:
Dr. Jitendra Gupta, Institute of Pharmaceutical Research, GLA University, Mathura-281406, Uttar Pradesh, India.
Phone: +91-8979136611
E-mail: smartjitu79@gmail.com

Received: 16-08-2025
Revised: 20-09-2025
Accepted: 28-09-2025

GRAPHICAL ABSTRACT

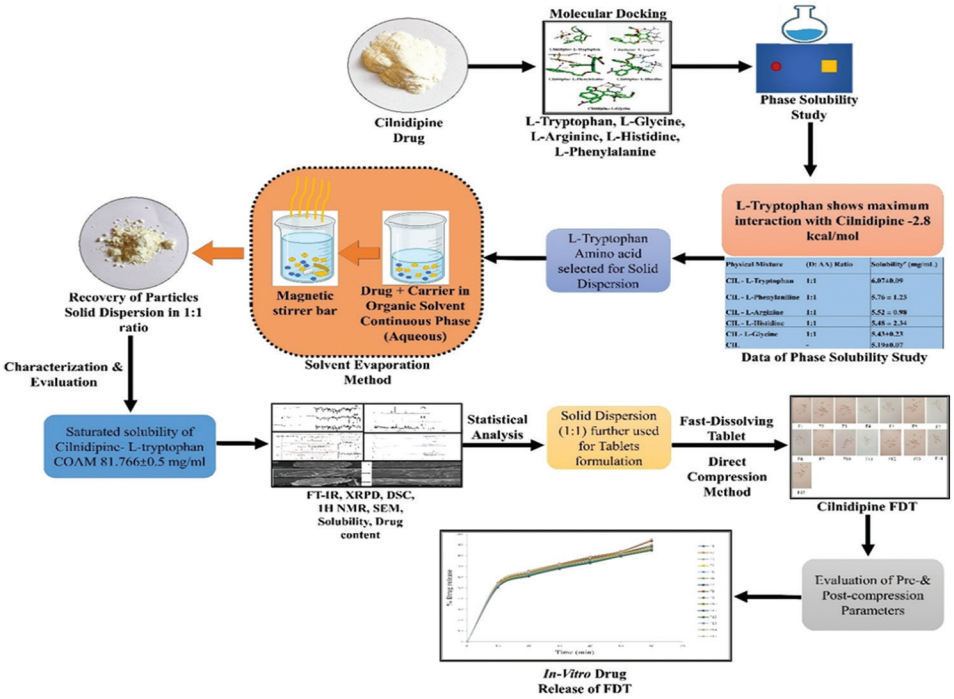

Cilnidipine co-amorphous solid dispersions: Insights from molecular docking and optimization fast-dissolving tablet

of hydrophilic carriers have shown improvement in the solubility and absorption, which results in drug dissolution.[4]

Cilnidipine (CIL), which is a fourth-generation calcium channel blocker and a BCS Class II drug, has shown similar challenges because of its low solubility and bioavailability (13%).[5] Its half-life is found to be 7.5 h, which exhibits the highest plasma concentration within 1.8–2.2 h when taken orally.[6] Improving CIL's solubility as well as bioavailability with SD techniques by amino acids (AAs) has shown results promising enough to overcome these limitations.[7]

The SD method involves the induction of an amorphous drug into a stabilizing excipient matrix.[8] This process leads to the inhibition of recrystallization, which allows the drug to remain in a high-energy, disordered state. This results in the enhanced solubility by achieving supersaturation in the gastrointestinal environment, and this ultimately improves the absorption as well as therapeutic efficacy.[9] Furthermore, the addition of AAs in SD formulations has shown to stabilize the amorphous state, which promotes better water interaction and faster dissolution rate.[10]

The pharmaceutical industries are increasingly recognizing the need for innovation to approach drug solubility enhancement and bioavailability.[11] Techniques like co-amorphous (COAM) SD, molecular complexation, and the use of hydrophilic carriers have shown alternatives to traditional methods.[12] Using modern formulation technologies, it is possible to improve the limitations of the poorly water-soluble drugs, which ensures the consistent therapeutic efficacy as well as improved patient compliance.

This study was conducted to improve the solubility as well as bioavailability of CIL through SD techniques combined with AAs. By addressing the solubility issues of the CIL, this research leads to the contribution in the broader field of pharmaceutical research and development, offering insights into the innovation of the drug delivery systems and leading the way for more effective treatments for poorly soluble drugs.

MATERIALS AND METHODS

Materials

CIL was procured as a gift sample (Relington Pharma, Ahmedabad), and L-tryptophan, L-arginine, L-histidine, L-glycine, camphor, croscarmellose sodium (CCS), lactose, cross-povidone, saccharine, mannitol, and talc were purchased from CDH Pvt. Ltd., India. All reagents were used are of analytical grade.

Methods

Preformulation studies

Molecular docking of CIL and AAs

The molecular docking mimics the atomic-level interaction of tiny molecules and proteins.[13] This leads to the exploration of

how small molecules interact with the binding sites of target AA, which results in facilitation, and the characterization of important chemical processes and improvement in the solubility of low water-soluble drugs. The docking process includes two important steps: Evaluation of the binding affinity and prediction of the shape of the ligand, position, as well as orientation in the binding site. Molecular docking is a computational method which is used in the prediction of the most favorable orientation of one molecule relative to another as they form a stable complex.[14] This approach is important in the drug discovery and design as it identifies and improves the prospective drug candidates by modeling their interactions with the target AA.[15] Use of the computational drug discovery software, such as Pymol, Pyrx, and Drug Discovery Studio (free version), analyze the interaction between pharmaceuticals and AAs to enhance the solubility of CIL (BCS class II). For the procedure of docking, SDF files were taken from PubChem and transferred into the protein data bank format by using Pymol software. Drug compounds are docked into an unknown AA binding site to improve the binding model by using the Pyrx virtual screening tool.

Saturated solubility studies of drug and physical mixture (PM)

The solubility of CIL was evaluated using a pharmacopeial method. CIL (100 mg) was added to 5 mL of distilled water and shaken reciprocally at 37°C for a period of 72 h. The solubility of the resulting solutions was analyzed by using a ultraviolet (UV) visible double-beam spectrophotometer (Shimadzu 1800, Japan) and compared with reference data. PM of AAs, as well as CIL (AA-CIL), was produced in an aqueous medium in a 1:1 molar ratio (AA and CIL). The molecular weight ratios of CIL to various AAs were as follows: CIL: L-tryptophan (123:51), CIL: L-glycine (123:18.75), CIL: L-phenylalanine (123:41.29), CIL: L-arginine (123:43.55), and CIL: L-histidine(123:38.79), and the components were thoroughly mixed.[16,17]

COAM formulation methods

Solvent evaporation method of COAM

CIL and AA (L-tryptophan) were weighed in a ratio of 1:1 and dissolved in ethanol according to their molecular weight. The solution was sonicated and stirred for 1h over a magnetic stirrer. After sonication, ethanol was evaporated using a water bath at 60°C until all solvent had evaporated. Finally, SD was dried, crushed, and passed through 100# sieves, and then stored in desiccators until further use. The dried bulk of the SD complex was prepared using the solvent evaporation process.[18-21]

Characterization of COAM formulations

Scanning electron microscopy (SEM)

Samples were analyzed using SEM (7610F Plus/JEOL, Peabody, Massachusetts, USA) at an 15 kV as an upsurge voltage. Before imaging, a sputter coater 108 auto (Cressington Scientific Instruments Ltd., Watford, United Kingdom) was used to coat the samples with gold under a vacuum in an argon atmosphere after they had been distributed on aluminum stubs using double-sided carbon adhesive tape.[22,23]

Saturated solubility of COAM formulations

The solubility investigation of the PM and SD was conducted using water as a solvent. Solubility studies on PM and SD were carried out using the shaking flask method. The generated SD was incorporated to 10 mL of water and then sonicated at 25°C ± 2°C for 10 min. The sample was shaken for 24 h in an orbital shaker before the flask was allowed to settle. After that, the supernatant has undergoes to centrifugation at 3000 rpm for 10 min and analyzed using a UV-visible double-beam spectrophotometer (Shimadzu 1800, Japan) to measure the absorbance at 260 nm to determine the solubility.[24,25]

^{1}H-nuclear magnetic resonance (^{1}H-NMR) study

Bruker, USA, used an Avance-III 400 MHz to record the ^{1}H-NMR spectra. Samples were prepared as a solution in a deuterated solvent, with the appropriate internal non-deuterated solvent peak ($CDCl_3$) used as a reference. Chemical shifts were measured in ppm (δ) relative to the $CDCl_3$peak. The characterization was conducted for the CIL, PM (CIL and L-tryptophan), and optimized COAM (CIL and L-tryptophan).[26,27]

Fourier transform infrared (FTIR) study

FTIR spectrophotometry determines the functional group and compatibility between the CIL and AA present. For FTIR measurements, the Shimadzu IR-SPRIT-T spectrometer (Shimadzu Corporation, Japan) with an attenuated total reflectance (ATR) accessory (Smart Endurance, single reflection ATR diamond composite crystal) was used to scan the CIL, PM (CIL and L-tryptophan), and optimized COAM samples from a range of 4000–400cm^{-1} and record the spectrum.[28,29]

Differential scanning calorimetry (DSC) study

DSC measurements were carried out using Discovery 25/TA Instruments Waters having a range of 90°–500°C (Waters, New Castle, DE 19720, USA). Under conditions of 50 mL/min nitrogen gas flow, thermograms were recorded. After being quickly chilled to −50°C for 15 min, around 5 mg of sample powder was put in an aluminum pan with a perforated cover. It was increased to 120°C at the pace of 10°C/min. All temperature data indicate the mean of three independent readings. The characterization was conducted for CIL, PM (CIL and L-tryptophan), and optimized COAM, and recorded the thermograms.[30]

X-ray powder diffraction (XRPD) study

XRPD analysis was conducted with a DIFFRAC. V3 SmartLab 3kW/Rigaku diffractometer (Rigaku diffractometer, Tokyo, Japan) with Cu Ka radiation (k 1.5 Å). The experiment was conducted using a current of 40 mA and an acceleration voltage of 50 kV. The samples were scanned at a speed of 0.13 2 h/s with a step size of 0.02 throughout a range of 5°–35° 2Θ. The DIFFRAC.V3 program (SmartLab

3kW/Rigaku, Tokyo, Japan) was used for data collection. The characterization was conducted for CIL, PM (CIL and L-tryptophan), and optimized COAM.[31]

Percent drug content

COAM (100 mg) was dissolved in 10 mL of ethanol. After the solution was filtered, a UV-visible double-beam spectrophotometer was used to detect the absorbance at 240 nm following an appropriate dilution.[32]

Optimization of selected factor using Box-Behnken design (BBD) for formulation of Fast-dissolving tablet (FDT)

The camphor (X_1), CCS (X_2), and cross-povidone (CP) (X_3) concentrations were the independent variables for the BBD. BBD was performed with three factors (X_1, X_2, and X_3), each at 3 levels (low [−1], medium [0], and high [+1]) to identify optimum levels Table 1. The model suggested fifteen experimental runs, and each factor was varied to optimize four different responses.

The time it took for the pill to disintegrate (Y1) and the percentage of medication release (Y2) were the dependent variables, or responses. Utilizing Design-Expert 13 software (Stat-Ease, Inc.), the mathematical model was confirmed by doing analysis of variance, calculating multiple correlation coefficients, and estimating the lack of fit.[33]

$$Y = \beta_0 + \beta_1 X_1 + \beta_2 X_2 + \beta_3 X_1^2 + \beta_4 X_2^2 + \beta_5 X_2 X_1 \quad (1)$$

Where Y represents the response, β_0 denotes the intercepts, X_1 and X_2 are the factors, and X_1 X_2 is the interaction term, X_{12} and X_{22} are the quadratic terms, and β_1, β_4, and β_5 are the associated coefficients.

Table 1: Independent variables and their levels

Independent variables and their levels			
Levels	**Camphor (mg)**	**CCS (mg)**	**CP (mg)**
−1	5	8	8
0	7.5	10	10
+1	10	12	12

Formulation of FDT of CIL-COAM

FDT has been prepared from each of the formulations. All the ingredients were individually sieved through a mesh (#60). The COAM and microcrystalline cellulose were blended by taking small portions of both at the same time and mixed them to obtain consistent mixture, which was then set aside. Subsequently, the other ingredients were weighed and mixed thoroughly. The tablets were directly compressed using punches to obtain tablets on a highly efficient single-station automatic tablet machine. All FDT (F1–F15) tablets were prepared in the same manner, as shown in Table 2.[34]

Evaluation parameter of blended powder of FDT

The powder flow properties were evaluated using several parameters. Dividing the bulk density by the tap density yields the Hausner ratio. Carr's index was determined by comparing the tapped and poured densities and observing the packing rate, using the formula:

Table 2: Formulation composition of FDTs of formulations F1F15

Formulation code	COAM (Mg)	Camphor (Mg)	CCS (Mg)	CP (Mg)	Saccharine (Mg)	Mannitol (Mg)	Talc (Mg)	Lactose (Mg)
F1	11.77	10	12	10	2.5	0.75	0.18	52.8
F2	11.77	7.5	8	8	2.5	0.75	0.18	61.3
F3	11.77	10	10	12	2.5	0.75	0.18	52.8
F4	11.77	7.5	10	10	2.5	0.75	0.18	57.3
F5	11.77	5	10	8	2.5	0.75	0.18	61.8
F6	11.77	5	12	10	2.5	0.75	0.18	57.8
F7	11.77	5	8	10	2.5	0.75	0.18	61.8
F8	11.77	5	10	12	2.5	0.75	0.18	57.8
F9	11.77	7.5	12	8	2.5	0.75	0.18	57.3
F10	11.77	7.5	12	12	2.5	0.75	0.18	53.3
F11	11.77	10	8	10	2.5	0.75	0.18	56.8
F12	11.77	7.5	10	10	2.5	0.75	0.18	57.3
F13	11.77	7.5	10	10	2.5	0.75	0.18	57.3
F14	11.77	7.5	8	12	2.5	0.75	0.18	57.3
F15	11.77	10	10	8	2.5	0.75	0.18	56.8

COAM (≡10 mg CIL)

$$Carr's\ index = (tapped\ density\text{-}poured\ density)/tapped\ density \times 100$$

The angle of repose (Θ) was assessed using the fixed funnel method, where a funnel was mounted on a stand at a predetermined height (h) above graph paper and placed on a flat surface. The sample was poured until the apex of the conical pile came into contact with the funnel tip. The radius (r) of the conical pile was measured to calculate as-

$$\Theta = tan\text{-}1\ (h/r)$$

Bulk density (ρ_b) was detected by putting powder into a graduated cylinder and dividing the weight by the volume, with the average of three measurements recorded. Tapped density (ρ_t) was calculated by tapping the cylinder containing a known weight of powder, dividing the powder weight by volume after tapping, and recording mean of three determinations.[35]

Evaluation parameter of FDT

FDT quality was assessed through various tests. Hardness was scaled by using a Pfizer-type hardness tester on 3 randomly selected tablets out of each formulation. Friability was evaluated using the Roche friabilator, where 20FDT were weighed before and after for 4 min at 25 rpm, and the % loss was determined by utilizing the formula:

$$\%\ friability = (initial\ weight\text{-}final\ weight)/initial\ weight \times 100$$

Variations in weight was determined by weighing 20 FDTs collectively and individually, comparing individual weights to the average to check for uniformity and determine the percentage variation as per United States Pharmacopeia (USP). Subsequently, all batches of FDTs were evaluated in the same manner.

Time of disintegration was measured by utilizing an apparatus for disintegration test (Electrolab, Mumbai) with a disintegrating medium (pH 1.2 buffer, 900 mL) at 37 ± 0.5°C. The disintegration time (sec) was noted for entire disintegration of FDT. The test was carried out in triplicate.

The percent drug content of FDT was analyzed by triturating, dissolving the drug into pH 1.2 buffer, and determination of the absorbance at 240 nm by utilizing an UV-visible spectrophotometer after specific dilution and determining concentration.[36]

In vitro drug release

For the dissolution study, FDT (≡10 mg CIL) was spun at 50 rpm using a paddle-type USP type-II apparatus (LAB INDIA DS 8000) in dissolution medium 1.2 pH buffer (900 mL) at 37 ± 0.5°C for 60 min. Then, the samples were taken at specific intervals of time (0,10,20, 30, 40, 50, 60 min) and maintained sink condition by adding PBS at the same time. After suitable dilution, the withdrawn sample was filtered through a 0.45 µm Whatman filter paper and analyzed at 240 nm using the buffer as a blank in a UV-Visible double-beam spectrophotometer (Shimadzu 1800, Japan). The batch that showed maximum drug release was considered an optimized FDT.[16]

RESULTS AND DISCUSSION

Molecular docking of CIL-AA binding affinities

Through the docking study, the binding affinities between CIL and different AAs (L-tryptophan, L-phenylalanine, L-histidine, L-arginine, and L-glycine) were evaluated. The results indicate that CIL exhibits the strongest interaction (binding affinity of −2.8 kcal/mol) with L-tryptophan, suggesting significant hydrophobic interactions and pi-stacking between the aromatic rings of the AA and the CIL shown in [Figure 1]. Similarly, CIL shows a strong affinity for L-phenylalanine (−2.7 kcal/mol) due to an aromatic ring capable of engaging in similar interactions. The interaction with L-Arginine (−2.1 kcal/mol) is moderate, likely due to the guanidinium group on arginine enabling electrostatic or hydrogen bonding interactions with CIL. L-histidine (−1.8 kcal/mol), with its imidazole ring, demonstrates weaker binding compared to aromatic AAs, possibly due to its more polar nature and lesser involvement in pi-stacking interactions. Finally, Glycine, the simplest AA, displays the weakest binding affinity (−1.3 kcal/mol), attributed to its lack of side-chain complexity, limiting its interaction potential with CIL. Overall, these results suggest that CIL binds more strongly to AAs with aromatic or complex side chains, with hydrophobic interactions and pi-stacking playing crucial

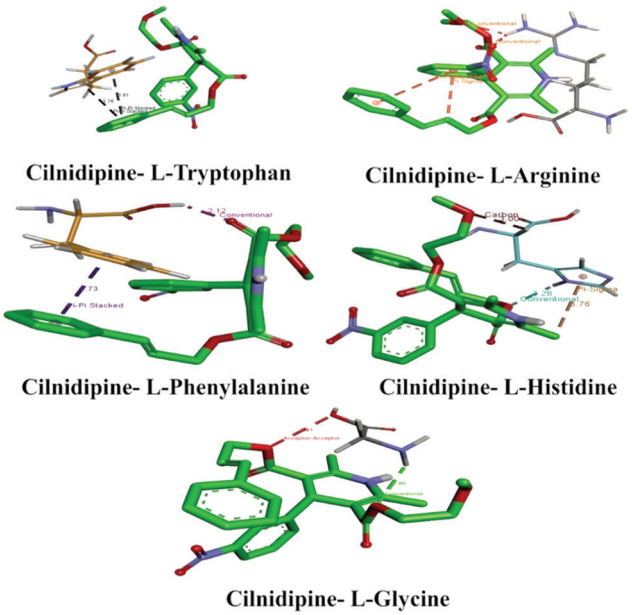

Figure 1: Molecular docking of Cilnidipine-amino acid binding complexes

roles in binding strength. Conversely, simpler or polar AAs exhibit weaker interactions with CIL.[15]

Saturated solubility data

CIL exhibited a solubility of 5.19 ± 0.07 mg/mL at absorbance maxima 240 (λ_{max}). When physically mixed with AAs in a 1:1 ratio, the solubility increased up to 6.07 ± 0.09 mg/mL with L-tryptophan, in contrast to other AAs. While PM of CIL with L-Phenylalanine showed solubility 5.76 ± 1.23 mg/mL, 5.52 ± 0.98 mg/mL with L-Arginine, and 5.48 ± 2.34 mg/mL with L-Histidine, respectively. Yet, the CIL-L-Glycine mixture showed the lowest solubility at 5.43 ± 0.23 mg/mL. These results indicate that the addition of AAs can enhance the solubility of CIL, with L-tryptophan providing the most notable improvement. Based on the saturated solubility data of the PM of the drug and AAs, L-tryptophan was chosen for further studies.[16,17]

In the case of a saturated solubility study of the amorphous mixture, the solvent evaporation method was utilized to prepare COAM using CIL and L-tryptophan. The solubility of COAM (CIL: L-Tryptophan 1:1) was enhanced 15.75-fold (81.766 ± 0.5 mg/mL) in comparison to CIL (5.19 ± 0.07 mg/mL) due to conversion of CIL into an amorphous form, and then confirmed by SEM study.

SEM

A SEM of COAM [Figure 2] at a magnification of ×1000 and ×5000 appeared like a rough, porous surface. The crystalline nature of CIL was converted into an amorphous form with diameters ranging from 1 to 10 µm. In addition, smaller particle size, expand surface area, near contact, which is aligned within the hydrophilic carrier and CIL, and the amorphous nature (COAM) likely contributed to the improved solubility and dissolution rate of CIL.[22,23]

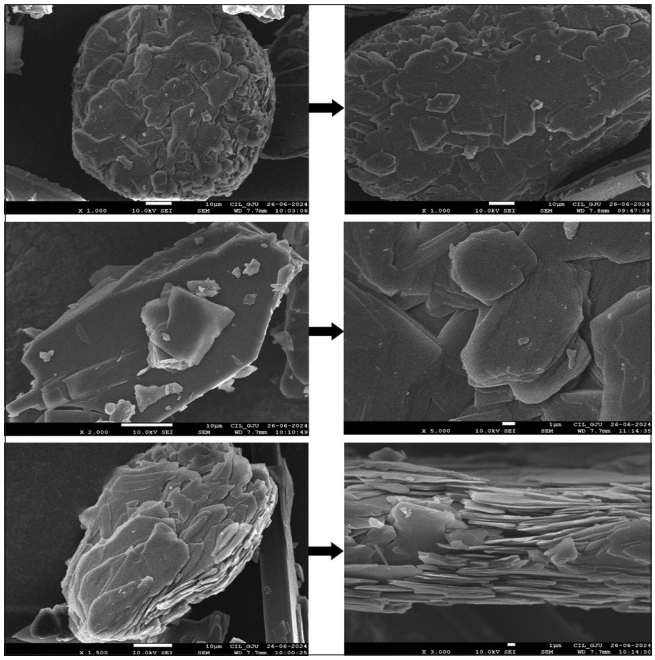

Figure 2: Scanning electron micrograph of co-amorphous at magnification power (1000–5000)

FTIR

The FTIR spectroscopy analysis was conducted to investigate drug carrier compatibility study on the CIL, PM, and COAM. IR spectra showed in [Figure 3], elucidates the characteristic peaks of CIL at 3283.99 cm^{-1}, due to N-H stretching (Aromatic 2° amine), peak at 1251.59 cm^{-1} of N=O (Nitroso), peak at 1346.32 cm^{-1} of -N-O (Nitro), peak at 1680.75 cm^{-1} of C=C stretching acyclic (Alkenes), and peak at 2945.26 cm^{-1} $-OCH_3$ (Methoxy).

IR spectrum of CIL and L-Tryptophan PM, showed characteristic peak at 3282.56 cm^{-1} of N-H stretching (Aromatic 2° amine), 1250.16 cm^{-1} of N=O (Nitroso), 1349.19 cm^{-1} of -N-O (Nitro), 1680.75 cm^{-1} of C=C stretching acyclic (Alkenes), and 2945.26 cm^{-1} of OCH_3 (Methoxy). COAM(CIL and L-Tryptophan) IR spectra showed peak at 3282.56 cm^{-1}, of N-H stretching (Aromatic 2° amine), 1250.16 cm^{-1} of N=O (Nitroso), 1349.19 cm^{-1} of -N-O(Nitro), 1680.75 cm^{-1} of C=C stretching acyclic (Alkenes), and 2945.26 cm^{-1} of $-OCH_3$ (Methoxy) results in indicating the presence of CIL in COMA. Unique peaks in the PM and formulation strongly suggest significant interactions with tryptophan. Furthermore, the observed shifts in peak positions and alterations in intensity unequivocally indicate notable chemical interactions, and lead COAM formation.[37]

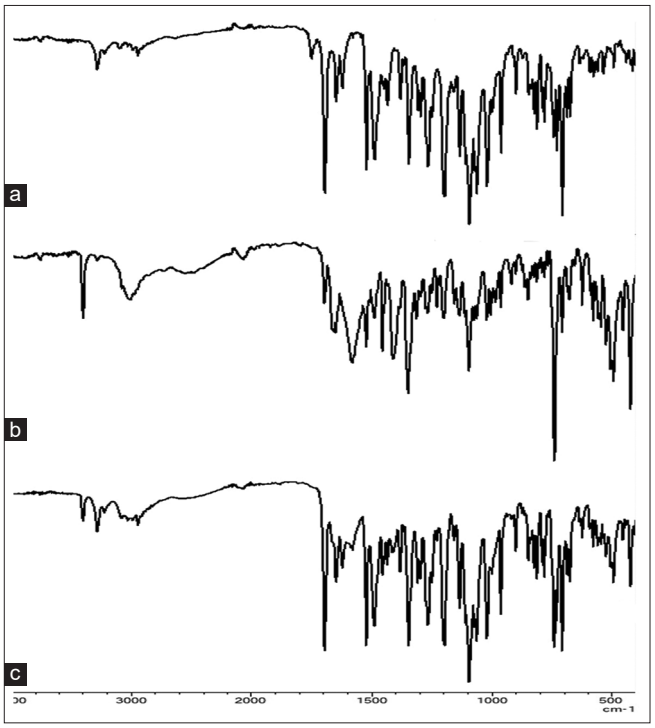

Figure 3: Fourier transform infrared graph of Cilnidipine (a), physical mixture (b), and co-amorphous (c)

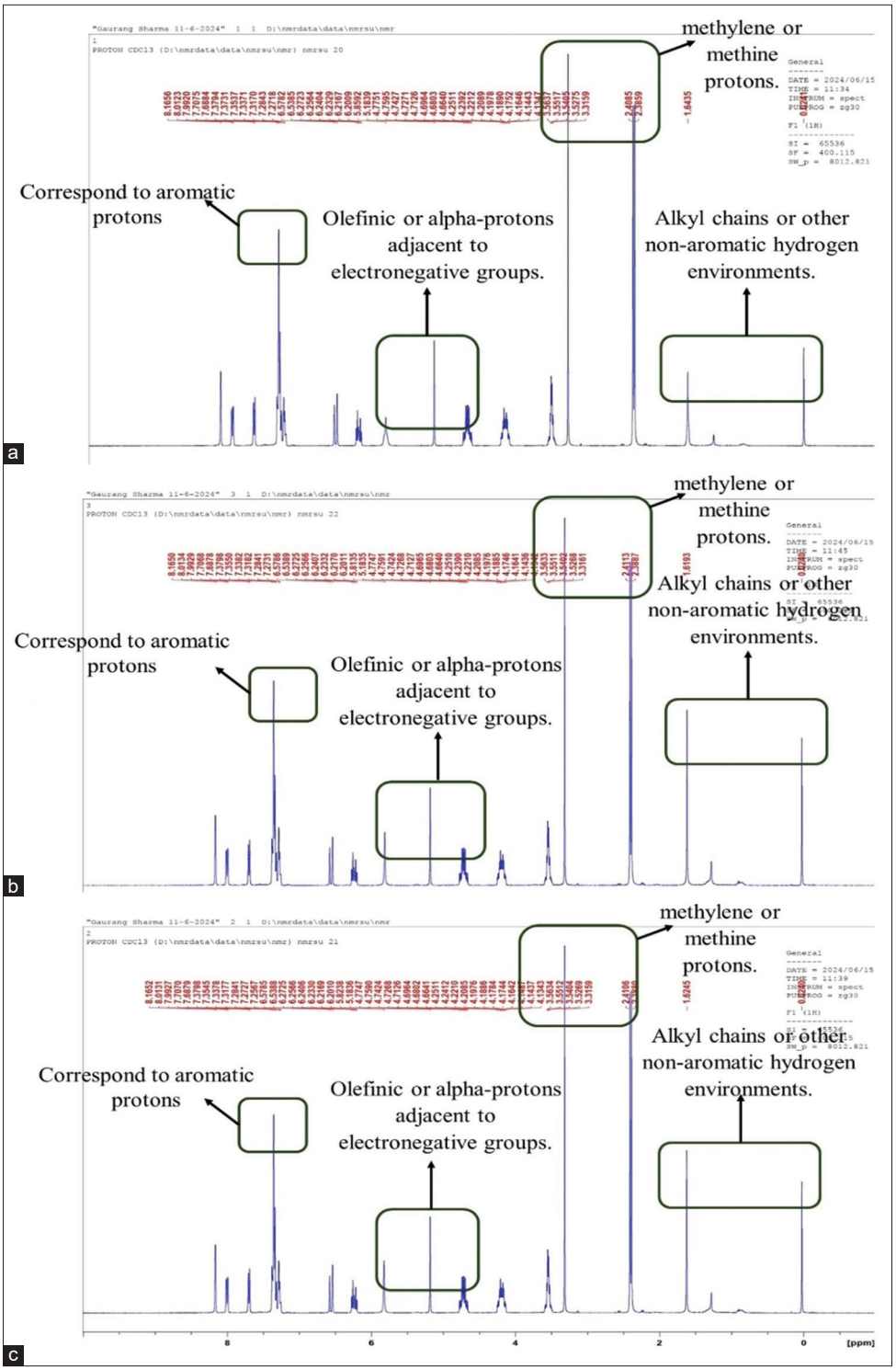

Figure 4: [1]H-nuclear magnetic resonance graph of Cilnidipine (a), physical mixture (b), and co-amorphous (c)

[1]H-NMR

The peaks in the high-field region (around 8–7 ppm) correspond to aromatic protons. Peaks in the mid-field region (around 6–4 ppm) are likely due to olefinic or alpha-protons adjacent to electronegative groups. The low-field region (around 4-2 ppm) peaks can be attributed to methylene or methine protons. The downfield region (around 3-0 ppm) peaks likely arise from alkyl chains or other non-aromatic hydrogen environments. The PM shows peaks identical to CIL, suggesting no significant interaction between CIL and L-tryptophan in the PM. The COAM formulation shows slight shifts in peaks compared to CIL, indicating possible interactions and changes in the chemical environment due to the formulation process. CIL displays a clear [1]H-NMR spectrum with defined peaks that correspond to its hydrogen

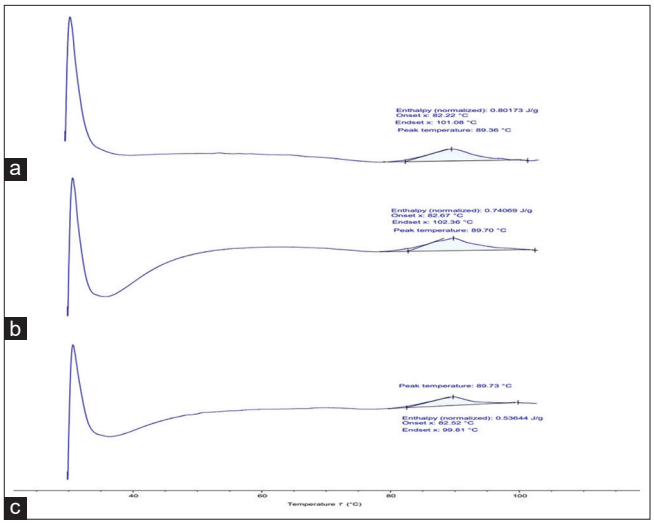

Figure 5: Differential scanning calorimetry thermograms of Cilnidipine (a), physical mixture (b), and co-amorphous (c)

atoms. The PM maintains the same peak positions as CIL, indicating that L-tryptophan minimally affects CIL's structure. Minor peak shifts [Figure 4] suggest potential interactions or environmental changes in CIL, likely enhancing CIL solubility due to COAM formulation.[26]

DSC

DSC study was performed to investigate the change in crystallinity. The thermograms of CIL, PM, and COAM provide the thermal transition information. In the thermogram of CIL, the normalized enthalpy was found to be 0.80173 J/g, with an onset temperature (82.22°C), an endset temperature (101.80°C), and a peak temperature of 89.36°C. For the thermogram of the PM, the normalized enthalpy was 0.74069 J/g, the onset temperature (82.92°C), the endset temperature (99.81°C), and the peak temperature 89.73°C. Finally, the thermogram of COAM showed a decrease in normalized enthalpy of 0.53844 J/g, an onset temperature (82.67°C), an endset temperature (102.36°C), and a peak temperature of 89.70°C,indicating distinct thermal behavior due to amorphous nature of COAM, showing variations in their phase transitions or thermal stability [Figure 5].[30]

XRPD

The XRPD diffractogram of CIL, PM, COAM was studied as shown in [Figure 6]. CIL exhibited a distinct, intense peak at 2Θ, indicative of its crystalline structure. In contrast, the PM containing CIL and L-tryptophan showed consistent and pronounced sharp peaks at 2Θ. It is a simple combination without a chemical reaction, and the XRPD pattern retains the crystalline peaks of pure CIL. Additional peaks may appear due to Tryptophan, reflecting its own crystalline structure. In contrast, the COAM containing CIL, L-tryptophan, and ethanol showed consistent and pronounced sharp peaks at

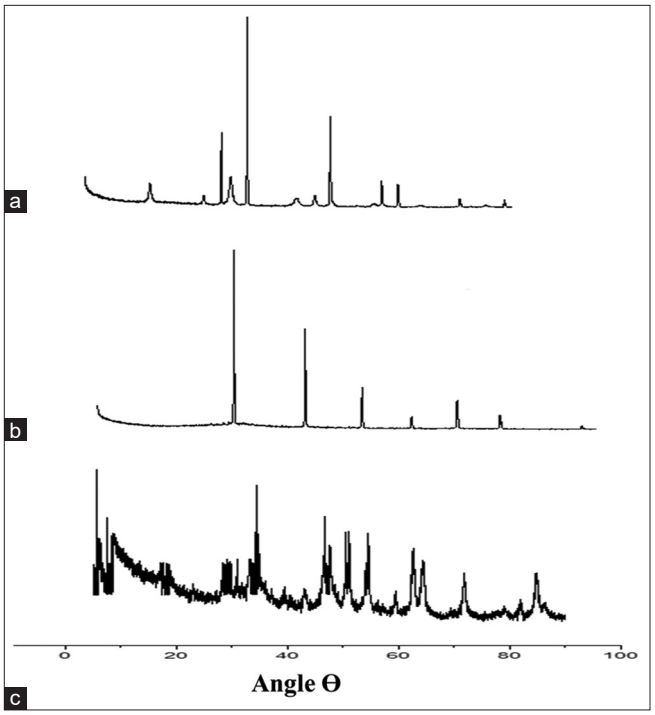

Figure 6: X-ray powder diffraction pattern of Cilnidipine (a), physical mixture (b), and co-amorphous (c)

2Θ. The addition of ethanol can cause partial dissolution of CIL and Tryptophan, leading to changes in their crystalline structures. Upon evaporation, the re-crystallization process can result in new or modified amorphous forms. This can lead to shifts in peak positions and changes in peak intensities in the XRPD pattern.[31]

Optimization of CIL- FDT using BBD

As an outcome of the optimization research, a BBD with three factors, two responses, and 15 runs was utilized. This experimental design consists of a set of points located at the midpoints of each edge of the multidimensional cube, along with replicates at the central point. From the experimental data, FDT formulated using BBD design exhibited a disintegration time of 69 s and an *in-vitro* drug release of 94.86 ± 0.29%, indicating its rapid and efficient action. The independent and dependent variables employed in the study are detailed in Table 3 and shown in [Figure 7].

Independent Variable: X_1- Camphor, X_2- CCS, X_3- CP

Dependent Variable: Y_1- Disintegration Time (sec), Y_2- *In vitro* drug release (%).

$$Y_1 = 70.67+3.62\ A+4.62\ B-1.00\ C+4.75\ AB+2.00\ AC-0.5000\ BC-1.71\ A^2+4.79\ B^2-1.46\ C^2$$

$$Y_2 = 85.97-1.18\ A-0.4425\ B+0.4538\ C+1.00\ AB-3.37\ AC-3.23\ BC-1.15\ A^2+1.40\ B^2+3.73\ C^2$$

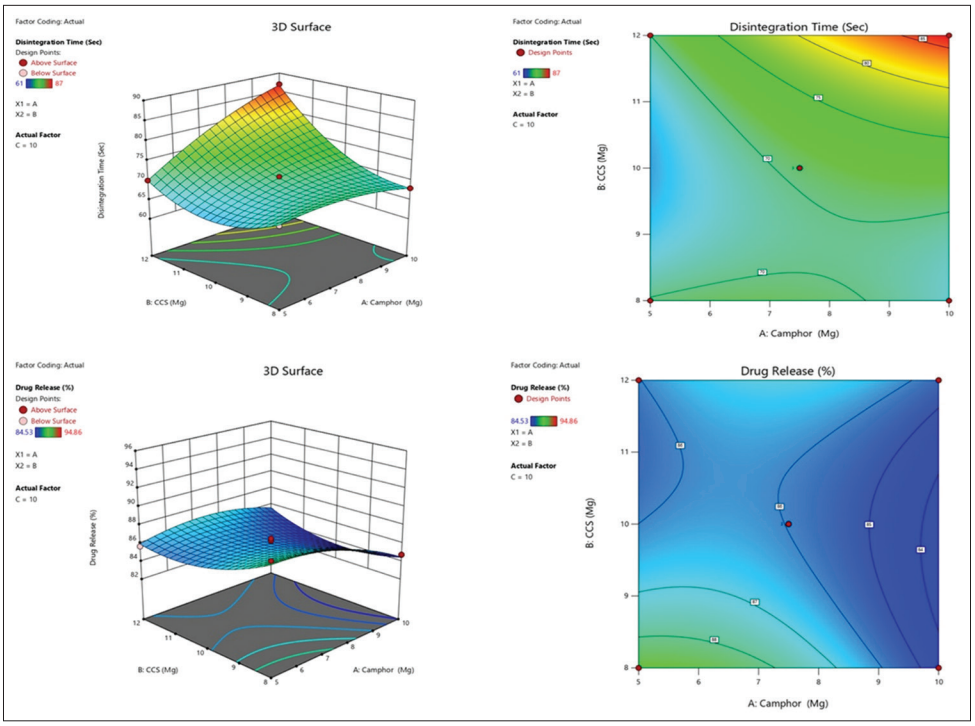

Figure 7: 3D response surface for the effect of X_1: Camphor X_2: croscarmellose sodium X_3: cross povidone on the response, Y_1 (Disintegration time sec), Y_2 (%Drug release)

Table 3: Box-Behnken experimental design of CIL-FDT

Run	Factor 1	Factor 2	Factor 3
	X: Camphor	X2: CCS	X3: CP
	(mg)	(mg)	(mg)
1	10	12	10
2	7.5	8	8
3	10	10	12
4	7.5	10	10
5	5	10	8
6	5	12	10
7	5	8	10
8	5	10	12
9	7.5	12	8
10	7.5	12	12
11	10	8	10
12	7.5	10	10
13	7.5	10	10
14	7.5	8	12
15	10	10	8

Optimized composition of CIL-FDTs

CIL-FDT (F14), Table 3, was developed using the direct compression method and stands out as the optimal choice. It showcases superior performance in terms of rapid disintegration, *in vitro* drug release, enhanced bioavailability, and patient compliance.

Characterization of CIL-FDT properties

Pre-compression characterization of the powder blend

The pre-formulation study of the powder blend indicated favorable flow properties, as evidenced by angle of repose values, a good compressibility index, and an appropriate Hausner's ratio. These results are summarized in Table 4. Specifically, F14 powder blend exhibited free-flowing characteristics, ensured the consistency in production of tablets with uniformity in weight. The experimental analysis of the F14 formulation yielded the following results: an angle of repose of 24.54 ± 0.31°, a bulk density of 0.43 ± 0.05 g/mL, a tapped density of 0.49 ± 0.11 g/mL, a Hausner's ratio of 1.13 ± 0.01, and a Carr's index of 12.26 ± 0.18% resulting in confirm the excellent flow properties of the powder mixture.[35]

Post-compression evaluations

The prepared drug met the content uniformity criteria outlined in the USP 31 specifications. Post-formulation analysis of the FDT demonstrated favorable parameters, including acceptable weight variation, hardness, friability, and thickness evaluation test, as summarized in Table 5. Specifically, the weight variation (10%) of the 100 mg FDT ranged from 99.69 ± 7.47 to 103.87 ± 6.25 mg, hardness ranged 2.48 ± 0.78 to 2.67 ± 0.56 kg/cm^2, friability <1%, thickness from 3.52 ± 0.14

Table 4: Pre-compression characterization of powder blended for CIL-FDT

Formulation codes	Bulk density[a] (g/mL)	Tapped density[a] (g/mL)	Hausner ratio[a]	Carr's index (%)	Angle of repose (°)
F1	0.41±0.05	0.48±0.12	1.17±0.02	14.58±1.42	30.28±0.42
F2	0.43±0.04	0.49±0.22	1.13±0.02	12.24±1.16	25.71±0.33
F3	0.38±0.02	0.45±0.14	1.18±0.01	15.56±0.86	26.93±0.58
F4	0.44±0.06	0.50±0.11	1.13±0.05	12.05±0.44	30.33±0.39
F5	0.42±0.05	0.49±0.10	1.16±0.02	14.20±3.42	25.61±0.49
F6	0.39±0.01	0.45±0.21	1.15±0.01	13.37±1.45	30.37±0.32
F7	0.40±0.07	0.47±0.14	1.17±0.05	14.83±0.16	28.28±0.38
F8	0.41±0.05	0.48±0.35	1.17±0.04	14.56±0.21	26.54±0.32
F9	0.45±0.05	0.52±0.20	1.15±0.05	13.43±3.10	25.54±0.33
F10	0.40±0.01	0.48±0.16	1.20±0.02	16.65±0.42	30.37±0.38
F11	0.38±0.06	0.45±0.27	1.18±0.08	15.57±1.86	30.54±0.58
F12	0.39±0.05	0.45±0.18	1.15±0.05	13.36±1.42	29.33±0.49
F13	0.42±0.04	0.48±0.23	1.14±0.09	12.57±0.16	26.54±0.38
F14	0.43±0.05	0.49±0.11	1.13±0.01	12.26±0.18	24.54±0.31
F15	0.42±0.04	0.48±0.10	1.14±0.07	12.57±1.41	27.50±0.33

[a]*n*=3 ± S.D

Table 5: Post-compression characterization of CIL-FDT

Formulation codes	Weight variation[a] (mg)	Hardness[a] (kg/cm²)	Friability[a] (%)	Thickness[a] (mm)	Drug content[a] (%)	Disintegration Time[a] (s)	Drug release[a] (%)
F1	99.69±7.47	2.65±0.45	0.45±0.04	3.52±0.14	95±0.15	87±1.12	85.21±0.16
F2	99.82±4.45	2.57±0.12	0.29±0.07	3.55±0.12	95±0.04	70±2.15	87.55±0.48
F3	99.79±5.74	2.58±0.52	0.47±0.05	3.57±0.12	95±0.14	72±1.01	84.53±0.28
F4	102.68±2.54	2.67±0.56	0.57±0.05	3.56±0.15	92±0.16	70±1.09	86.58±1.42
F5	99.89±4.48	2.55±0.55	0.18±0.04	3.52±0.18	93±0.02	67±1.00	85.83±0.65
F6	99.77±2.65	2.45±0.46	0.41±0.05	3.55±0.16	92±0.19	70±2.03	85.68±1.85
F7	103.87±6.25	2.59±0.26	0.27±0.06	3.53±0.17	93±0.06	70±2.10	89.23±0.45
F8	99.92±2.98	2.57±0.35	0.25±0.08	3.59±0.17	98±0.05	69±1.07	93.53±1.21
F9	102.55±4.14	2.62±0.85	0.37±0.06	3.54±0.18	94±0.02	80±1.14	93.79±0.35
F10	99.97±2.55	2.54±0.55	0.52±0.05	3.58±0.19	97±0.16	77±1.18	88.18±0.24
F11	102.19±3.25	2.65±0.64	0.47±0.02	3.59±0.15	95±0.14	68±1.10	84.76±0.15
F12	99.73±6.26	2.65±0.58	0.35±0.03	3.55±0.16	95±0.19	71±2.06	85.03±0.31
F13	99.80±5.24	2.48±0.78	0.15±0.04	3.54±0.15	96±0.16	71±1.01	86.3±0.27
F14	99.95±4.65	2.58±0.95	0.18±0.05	3.56±0.14	99±0.78	61±2.02	94.86±0.29
F15	99.79±8.75	2.55±0.55	0.51±0.02	3.53±0.11	95±0.25	70±1.11	90.30±0.48

[a]*n*=3 ± S.D

to 3.59 ± 0.15 mm, and 92 ± 0.16 to 99 ± 0.78% drug content and disintegration time 61 ± 2.02–87 ± 1.12 s. Among all the batches, F14 demonstrated the most favorable post-compression properties, highest drug content 99 ± 0.78%, and disintegration time 61 ± 2.02 s, as shown in Table 5.[36,38-40]

In vitro drug release

In vitro dissolution studies of formulations F1 to F15 showed drug release ranging from 84.53 ± 0.28% to 94.86 ± 0.29% within 60 minutes from the FDTs, compared to only 36.27% from pure CIL and acceptable according to the USP, attributed to the incorporation of the superdisintegrant sodium starch glycolate, which disintegrated the FDTs within 61 ± 2.02 s, significantly enhancing drug release in a short time. Among all formulations, F14, comprising CIL and L-tryptophan at the highest concentration, exhibited the best performance, achieving the highest drug release shown in [Figure 8].[16,41,42]

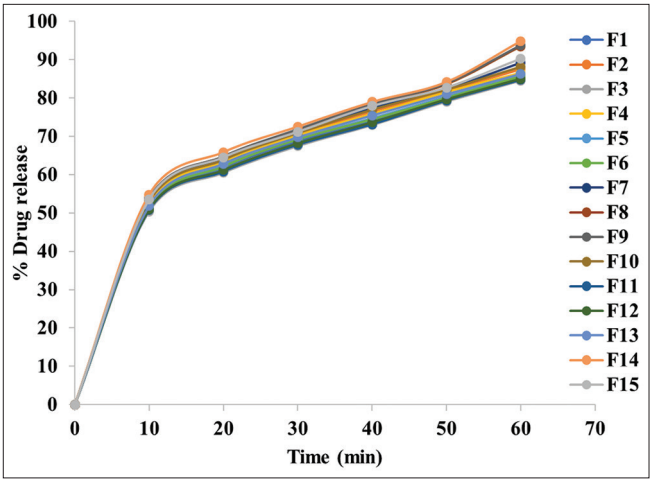

Figure 8: Percentage drug release of co-amorphous-fast-dissolving tablet from F1 to F15

CONCLUSION

This study investigated COAM formulations of the CIL with AA L-tryptophan prepared by solvent evaporation. On a general basis, this study confirms the assumption that AAs are generally promising excipients for the formation of co-amorphous mixtures. The FDT formulation was optimized by BBD with three factors and two responses utilized to investigate the impact of formulation on response, such as disintegration time and % drug release. The findings revealed that the factors camphor, CP, and CCS all had an impact on the response variables. CIL-FDTs were developed to provide an interesting field for further research, given that results may be extrapolated to different drugs, for which a rapid onset of action is an attractive target.

ETHICAL APPROVAL AND CONSENT TO PARTICIPATE

No need for ethical approval because there is no *in vivo* activity performed.

CONSENT FOR PUBLICATION

All authors agree to publish this article in Asian Journal of Pharmaceutics.

DATA AVAILABILITY

The data and material will be provided by the corresponding author upon reasonable request.

AUTHOR CONTRIBUTIONS STATEMENT (CREDIT FORMAT)

Mr. Gaurang Sharma (GS): Original Draft, Language, Figures, Tables, Data curation. Jitendra Gupta (JG): Reviewing, Editing, Conceptualization.

ACKNOWLEDGMENT

The authors want to acknowledge the Institute of Pharmaceutical Research, GLA University, Mathura, for providing the necessary facilities.

REFERENCES

1. Loftsson T, Brewster ME. Pharmaceutical applications of cyclodextrins: Basic science and product development. J Pharm Pharmacol 2010;62:1607-21.
2. Tsume Y, Mudie DM, Langguth P, Amidon GE, Amidon GL. The biopharmaceutics classification system: Subclasses for *in vivo* predictive dissolution (IPD) methodology and IVIVC. Eur J Pharm Sci 2014;57:152-63.
3. Duong TV, Nguyen HT, Taylor LS. Combining enabling formulation strategies to generate supersaturated solutions of delamanid: *In situ* salt formation during amorphous solid dispersion fabrication for more robust release profiles. Eur J Pharm Biopharm 2022;174:131-43.
4. Bi Y, Xiao D, Ren S, Bi S, Wang J, Li F. The binary system of ibuprofen-nicotinamide under nanoscale confinement: From cocrystal to coamorphous State. J Pharm Sci 2017;106:3150-5.
5. Al Hazzaa SA, Rajab NA. Cilnidipine nanocrystals, formulation and evaluation for optimization of solubility and dissolution rate. Iraqi J Pharm Sci 2023;32:127-35.
6. Chakraborty RN, Langade D, More S, Revandkar V, Birla A. Efficacy of cilnidipine (L/N-type calcium channel blocker) in treatment of hypertension: A meta-analysis of randomized and non-randomized controlled trials. Cureus 2021;13:e19822.
7. Sapkal SB, Adhao VS, Thenge RR, Darakhe RA, Shinde SA, Shrikhande VN. Formulation and characterization of solid dispersions of etoricoxib using natural polymers. Turk J Pharm Sci 2020;17:7-19.
8. Budiman A, Handini AL, Muslimah MN, Nurani NV, Laelasari E, Kurniawansyah IS, *et al*. Amorphous solid dispersion as drug delivery vehicles in cancer. Polymers (Basel) 2023;15:3380.
9. Gan Y, Baak JP, Chen T, Ye H, Liao W, Lv H, *et al*. Supersaturation and precipitation applicated in drug delivery systems: Development strategies and evaluation approaches. Molecules 2023;28:2212.
10. Guinet Y, Paccou L, Hédoux A. Mechanism for

stabilizing an amorphous drug using amino acids within co-amorphous blends. Pharmaceutics 2023;15:337.
11. Bhalani DV, Nutan B, Kumar A, Singh Chandel AK. Bioavailability enhancement techniques for poorly aqueous soluble drugs and therapeutics. Biomedicines 2022;10:2055.
12. Das T, Mehta CH, Nayak UY. Multiple approaches for achieving drug solubility: An *in silico* perspective. Drug Discov Today 2020;25:1206-12.
13. Rosell M, Fernández-Recio J. Docking-based identification of small-molecule binding sites at protein-protein interfaces. Comput Struct Biotechnol J 2020;18:3750-61.
14. Mohanty M, Mohanty PS. Molecular docking in organic, inorganic, and hybrid systems: A tutorial review. Monatsh Chem 2023;154:683-707.
15. D'Souza S, Prema KV, Balaji S, Shah R. Deep learning-based modeling of drug-target interaction prediction incorporating binding site information of proteins. Interdiscip Sci 2023;15:306-15.
16. Mohana M, Vijayalakshmi S. Development and characterization of solid dispersion-based orodispersible tablets of cilnidipine. Beni Suef Univ J Basic Appl Sci 2022;11:83.
17. Sakure K, Kumari L, Badwaik H. Development and evaluation of solid dispersion based rapid disintegrating tablets of poorly water-soluble anti-diabetic drug. J Drug Deliv Sci Technol 2020;60:101942.
18. Yun TH, Lee JG, Bang KH, Cho JH, Kim KS. A quaternary solid dispersion system for improving the solubility of olaparib. Solids 2025;6:1.
19. Hassnain FU, Bashir S, Asad M, Nazir I, Qamar S, Hafiz MI, *et al*. Formulation and characterization of solid dispersion of nisoldipine by solvent evaporation method. J Pharm Altern Med 2012;2:21-8.
20. Alali AS, Muqtader Ahmed M, Fatima F, Anwer K, Ibnauf M, Aboudzadeh A. Chitosan-based spray-dried solid dispersions of apigenin in a 3D printable drug delivery system. J Appl Polym Sci 2025;142:e56310.
21. Qiu C, Zhang Y, Fan Y, Li S, Gao J, He X, *et al*. Solid dispersions of genistein via solvent rotary evaporation for improving solubility, bioavailability, and amelioration effect in HFD-induced obesity mice. Pharmaceutics 2024;16:306.
22. Nitta Y, Sato H, Yamamoto R, Imanaka H, Ishida N, Imamura K. Flavor retention characteristics of amorphous solid dispersion of flavors, prepared by vacuum-foam- and spray-drying under different conditions. Dry Technol 2024;42:227-37.
23. Zhang S, Wang H, Zhao X, Xu H, Wu S. Screening of organic small molecule excipients on ternary solid dispersions based on miscibility and hydrogen bonding analysis: Experiments and molecular simulation. AAPS PharmSciTech 2024;25:21.
24. Liu L, Ouyang F, Li T, Wen M, Zha G, Chen L, *et al.* Ternary solid dispersion of celecoxib produced by the solvent method with improved solubility and dissolution properties. Pharm Chem J 2024;57:1627-36.
25. Deshmane S, Kendre K, Deshmane S, Jain S, Sawant A, Solanki H. Utilizing phospholipid as an amphiphilic carrier for solid dispersion of ambrisentan: Formulation and evaluation. J Dispers Sci Technol 2024;July:1-9.
26. Okada K, Ono T, Hayashi Y, Kumada S, Onuki Y. Use of time-domain NMR for (1)H T(1) relaxation measurement and fitting analysis in homogeneity evaluation of amorphous solid dispersion. J Pharm Sci 2024;113:680-7.
27. Lale AS, Sirvi A, Debaje S, Patil S, Sangamwar AT. Supersaturable diacyl phospholipid dispersion for improving oral bioavailability of brick dust molecule: A case study of aprepitant. Eur J Pharm Biopharm 2024;197:114241.
28. Paudwal G, Dolkar R, Perveen S, Sharma R, Singh PP, Gupta PN. Third generation solid dispersion-based formulation of novel anti-tubercular agent exhibited improvement in solubility, dissolution and biological activity. AAPS J 2024;26:52.
29. Rosiak N, Tykarska E, Cielecka-Piontek J. Enhanced antioxidant and neuroprotective properties of pterostilbene (resveratrol derivative) in amorphous solid dispersions. Int J Mol Sci 2024;25:2774.
30. Dhuri A, Kanp T, Sarma AV, Nair R, Paul P, Sharma B, *et al.* Fabrication of amorphous solid dispersion of entacapone for enhanced solubility and dissolution rate: Morphology, solid state characterization, *in silico* molecular docking studies. J Mol Struct 2025;1324:140851.
31. Park JH, Kim IW. Polymeric additives to sustain the dissolution enhancement of niclosamide nanocrystals formed via freeze drying. J Cryst Growth 2025;649:127926.
32. Patel K, Kevlani V, Shah S. A novel posaconazole oral formulation using spray dried solid dispersion technology: *In-vitro* and *in-vivo* study. Drug Deliv Transl Res 2024;14:1253-76.
33. Elsayed MM, Aboelez MO, Elsadek BE, Sarhan HA, Khaled KA, Belal A, *et al*. Tolmetin sodium fast dissolving tablets for rheumatoid arthritis treatment: Preparation and optimization using box-behnken design and response surface methodology. Pharmaceutics 2022;14:880.
34. Eisa AM, El-Megrab NA, El-Nahas HM. Formulation and evaluation of fast dissolving tablets of haloperidol solid dispersion. Saudi Pharm J 2022;30:1589-602.
35. Bavaskar KR, Pote S, Vidhate P, Patil V, Jain A. Preparation and evaluation of mouth dissolving tablet of albendazole using different concentrations of super-disintegrant. J Fundam Appl Pharm Sci 2024;4:81-92.
36. Desai J, Dhameliya P, Patel S. Optimizing critical quality attributes of fast disintegrating tablets using artificial neural networks: A scientific benchmark study. Drug Dev Ind Pharm 2024;50:995-1007.
37. Ojarinta R, Heikkinen AT, Sievänen E, Laitinen R. Dissolution behavior of co-amorphous amino acid-indomethacin mixtures: The ability of amino acids to stabilize the supersaturated state of indomethacin. Eur J

Pharm Biopharm 2017;112:85-95.
38. Gupta J, Sorout R. Solid Dispersion Formulations Comprising Sulfamerazine. Indian Patent 202211017863 A. Available from: https://iprsearch.ipindia.gov.in/PatentSearch/PatentSearch/ViewApplicationStatus [Last accessed on 2025 Jul 05].
39. Gupta J. Mouth dissolving tablets: An insightinto challenges and future prospectsof technologies in pharmaceuticalindustries. Research J Pharm Tech 2022;15:5068-77.
40. Murti Y, Agrawal KK, Semwal BC, Gupta J, Gupta R. A review on novel herbal drug delivery system and its application. Curr Tradit Med 2023;9:43-55.
41. Gupta J, Sharma B, Sharma SK, Gupta P, Yadav R, Pawar N, *et al.* Hydrotropic solubilization: A novel approach for enhancing dissolution of antiemetic drugs in mouth dissolving tablets. Rev Electron Vet 2024;25:2270-7.
42. Gupta J, Gupta R. Effect of hydrophilic carriers for solubility and dissolution enhancement of sulfamerazine by solid dispersions technique. J Pharm Res Int 2021;33:313-26.

Source of Support: Nil. **Conflicts of Interest:** None declared.